ISSN: 0976-3031

Available Online at http://www.recentscientific.com

CODEN: IJRSFP (USA)

International Journal of Recent Scientific Research
Vol. 10, Issue, 07(C), pp. 33515-33523, July, 2019

International Journal of Recent Scientific Research

DOI: 10.24327/IJRSR

Research Article

ASSESSMENT OF ADSORPTION EFFICIENCY OF Ni(II) IONS FROM AQUEOUS SOLUTION BY MESOPOROUS ALUMINO SILICATE SYNTHESIZED FROM NATURAL HYDRATED SODIUM CALCIUM ALUMINO SILICATE

Vidhya Lakshmanaperumal[1]* and Dhandapani Munusamy[2]

[1]Department of Chemical Engineering, Sethu Institute of Technology, Kariyapatti - 626 106, Virudhunagar, Tamil Nadu, India

[2]Department of Chemistry, Sri Ramakrishna Mission Vidyalaya College of Arts and Science, Coimbatore 641-020, Tamil Nadu, India

DOI: http://dx.doi.org/10.24327/ijrsr.2019.1007.3686

ARTICLE INFO

Article History:
Received 4th April, 2019
Received in revised form 25th May, 2019
Accepted 18th June, 2019
Published online 28th July, 2019

Key Words:

FT-IR, Isotherm, Kinetics, Mesolite, SEM,TEM, Nickel adsorption.

ABSTRACT

Natural hydrated sodium calcium alumino silicate (mesolite) is an important and widespread industrial material of unique chemical structure. This study reports batch adsorption analysis of divalent nickel Ni(II) on mesolite. Removal efficiency of the mesolite was influenced by pH, initial Ni(II) concentration and adsorbent dose. The adsorption of Ni (II) by the mesolite was the highest at pH 7 and using a dosage of 0.05 g. The optimized concentration was 100 ppm. The order of the Ni(II) adsorption and adsorption isotherms were determined by varying parameters such as pH, initial concentration and contact time. Langmuir, Freundlich, Temkin models were applied to adsorption equilibrium data to find the best model. Langmuir model with $R^2 = 0.99$is the best fit for the adsorption data. The kinetics of adsorption followed pseudo first order reversible reaction as well as Intra particle diffusion method. The separation parameter, RL value was less than 1 which indicates that adsorption of Ni(II) on mesolite is favored. Mesolite was characterized by Fourier transform infrared analysis. Scanning electron microscopy and Transmission electron microscopy were used to analyze before and after adsorption. These results show that natural mesolite hold great potential to remove Ni(II) from industrial wastewater.

INTRODUCTION

Heavy metal contamination in the aquatic system is a big threat to the environment and it prevents the beneficial use of the surface water and groundwater bodies. Nickel is one of the heavy metal - micro nutrients needed in the body, but when taken in high dosages, it can cause serious health problems like birth defects, embolism, and chronic bronchitis. So it is necessary to remove the excess nickel ions by any efficient technology. The conventional technologies comprise of precipitation, electrolysis, biodegradation, adsorption, chemical coagulation and photo catalysis, ion exchange, reverse osmosis and filtration (Gönenand Önalan., 2016). These methods have numerous disadvantages such as being costly, generating secondary pollutants like sludge, and ineffective intreating effluents with low metal concentrations. The use of several natural products like chitosan, zeolite, banana pith, rice husk, and peat has proved to be an effective way due to non-toxicity, eco-friendly nature and availability of these adsorbents (Cybelle *et al*., 2011). Mesolite, a hydrated alumino silicate mineral contains alkali and alkaline-earth materials. Its unique porous nature makes it useful in adsorption, catalysis, ion exchange, petrochemical cracking and removal of gas and solvents. Mesolite is also found to be efficient in the adsorption of heavy metals from the waste water. Hence, the consumption of mesolite, a member of zeolites group, in a variety of fields has grown progressively (Lata *et al*., 2015). Mesolite has a three-dimensional crystalline structure which is rigid, consists of a network of interconnected tunnels and cages. Mesolite have the general chemical formula of $(M^+, M^{2+})O.Al_2O_3.xSiO_2.yH_2O$,where M^+ is usually Na^+ or K^+ ion and M^{2+} is Mg^{2+} or Ca^{2+} or Fe^{2+} ion; x and y are the total number of tetrahedrons per unit cell (Erdem *et al*., 2004). The heavy metal cations like lead, copper, cadmium and chromium can go into the structure of mesolite when they come into contact. Mesolite minerals have high cation-exchange capacity, high specific surface areas and rigid framework. Themicro pores, large volumeand high thermo stability of mesoliteare useful in purification of water and soil remediation (Franus and Wdowin 2010, Huang *et al*., 2014). Therefore, this study

Corresponding author:* **Vidhya Lakshmanaperumal
Department of General Surgery, Krishna Institute of Medical Sciences, Karad

reports the optimization studies on the efficiency of mesolite adsorbent in removal of Ni(II) ion with different Ni(II) concentration, pH, contact time, and dosage of the adsorbent.

MATERIALS AND METHODS

The mesolite used in the batch experiments was procured from Virbac SA. After washing with deionized water, it was dried at 105^0 C for 2 hours**.** Mesolite was used in the powdered formfor all the experiments. A stock solution of Ni (II) (1000 mg L^{-1}) was prepared by dissolving 4.478 g $NiSO_4.6H_2O$ in deionized water.

Characterization of mesolite

Evaluation of the surface charge of the mesolite with respect to pH, zeta potential tests was carried out by using the nano particle analyzer (Horiba Scientific, Japan). About 0.5 g of mesolite was suspended in 20 ml aliquots of buffer solutions with pH of 4, 5,6,7,8 and 9 and was allowed to settle for about 30 min (Vidhya *et al*., 2016). The samples were then fed into the analyzer. The analysis was repeated in triplicate. The mobility, zeta potential and conductance data were obtained from the result. The Fourier- Transform infrared spectra of the mesolite before and after adsorption of 100 mg L^{-1}Ni(II) at pH 7 were recorded using a Shimadzu, Model 8400S FT-IR spectrometer in the range 4000-400 cm^{-1}. FT-IR spectral data were used to probe the changes in vibrational frequencies of the functional groups present in the mesolite due to Ni(II) adsorption (Rohama *et al*., 2014). The morphological surface of the adsorbent was observed by a Quanta FEI 250 scanning electron microscope. The logarithmic phase cells both interacted and non-interacted were analyzed microscopically. A small amount of mesolite powder was taken in a 10 mm metal stub using carbon tape (Shah and Tokeer Ahamed, 2013). The samples were taken and made to sputter coated with gold in argon atmosphere under vacuum. The elemental analysis of both Ni(II) interacted and non-interacted mesolite was carried out by Energy Dispersive X-ray spectroscopy (EDAX). The sputtered gold samples were analyzed and the spectra were recorded using Quanta FEI 250 equipment. Transmission Electron Microscopic (TEM) image of mesolite adsorbent was recorded in a Hitachi Make: H-7650 model TEM instrument. The images were obtained in imaging mode using HV=80 KV and at magnification 3x105.

Batch adsorption studies

Batch adsorption studies were conducted by adding 0.05g of mesolite in different 100 ml Erlenmeyer flasks containing 50 ml of different concentrations (50-250 mg L^{-1}) of nickel solution. The flask containing the solution mixture was well shaken at 100 rpm for 120 min by an orbital shaker at 25^0C.The effect of contact time on batch experiments was examined by varying the contact time of suspensions from 0 to 120 min. Then the concentrations of unadsorbed Ni(II) were determined by colorimetric method with 0.5% dimethyl glyoximereagent in a colorimeter (Hach Make: DR/2400 model) at 470 nm. Experimental variables taken into consideration were (i) the effect of pH (2 to 8) on the adsorption capacities, (ii) dosage of mesolite (0.05 to 0.25 g), (iii) and initial nickel concentration (50 to 250 mg L^{-1}).

Adsorption capacity

The adsorption capacity was calculated at equilibrium (qe) (Dajana *et al*., 2014). The removal percentage (R %) of divalent nickel was calculated for each turn as follows.

$$R(\%) = \frac{C_O - C_e}{C_o} * 100 \quad \text{--1}$$

where C_o and $C_e$represent the initial and equilibrium concentrations of nickel ion in aqueous solution. The adsorption capacity for each concentration of nickel ((II) at equilibrium was determined by the following expression (Cheraghi *et al*., 2015; Raziyeh Zandipak and Soheil Sobhanardakani *et al*., 2016).

$$Adsorption\ capacity = qe\ \frac{(mg)}{(g)} = \frac{Co - Ce}{m*V} \quad \text{--2}$$

where V is the volume of solution in litre and m is the mass of the adsorbent used in grams.

Optimization of adsorption of Ni(II) over mesolite

The effect of Ni (II) concentration, mesolite dosage, pH and contact time were analyzed to optimize the best adsorption condition. The adsorption of nickel ions onto coirpith biochar was studied by varying the adsorbent quantity (0.01, 0.02,0.03,0.04, 0.05g) in the test solution while keeping the initial nickel ion concentration (100 mg L^{-1}), temperature (25 ± 1°C) and pH(7) constant at all different time intervals. In the next set of experiments, the adsorbent dosage was fixed as 0.05 g and metal concentration100 mgL^{-1}, pH was varied from 2 to 8**.** The solution pH was adjusted using 0.5$molL^{-1}$HCl or 0.5$molL^{-1}$ NaOH. By keeping the adsorbent dosage as 0.05g and pH 7, concentration of metal ions (50 to 250 mg L^{-1}) was varied. In every trial, after adsorption, the sorbate was decanted and separated from the sorbent by centrifugation and the supernatant liquid was analyzed for the residual metal concentration. The residual carbon is further used for subsequent studies. Batch experiments were performed in triplicate and average values are presented. The concentrations of the samples were determined by using a calibration graph.

Adsorption Isotherms

The interaction of sorbate molecules with the sorbent can be explained by adsorption isotherms. The Langmuir, Freundlich and Temkin isotherms were used to find a reasonable model to suit the adsorption equilibrium data at 27 ± 1^0C.The isotherms help to study the mode of interaction of Ni(II)ions with mesolite when they are in equilibrium. Langmuir (equation 1) Freundlich (equation 2) Temkin (equation 3) isotherms were plotted by using standard straight-line equations.

$$\frac{Ce}{qe} = \frac{Ce}{Q_{max}} + \frac{1}{b * Q_{max}} \quad --3$$

where, qe (mgg^{-1}) is the equilibrium adsorption capacity and Ce (mgL^{-1}) is the concentration of Ni(II) ions at equilibrium. Q_{max}(mg g^{-1}) is the maximum capacity of the metal ion monolayer and b (L mg^{-1}) refers the adsorption equilibrium constant. Q_{max} and b can be determined from a linear plot (Seliem and Komarneni 2016; Langmuir 1918).

$$\log qe = \log Kf + (\frac{1}{n}) \log Ce \quad --4$$

where, Kfis the Freundlich constant correlated to the sorption capacity (mg g^{-1}) ,Ce (mgL^{-1}) is the concentration of Ni(II) ions at equilibrium , qe (mgg^{-1}) is the equilibrium adsorption capacity and n is the heterogeneity factor. K_f and n can be determined from a linear plot of log qe against log Ce (Nurzulaifa Shaheera Erne *et al* 2016; Freundlich 1906).

$$qe = B \ln K_t + B \ln Ce \quad --5$$

Where C_e is the equilibrium concentration of a metal in solution (mg L^{-1}), $q_e$is the amount of Ni(II) ions adsorbed onto the mesolite (mg g^{-1}). *B*is the Tempkin constant that relates to the heat of sorption. Mathematically, B= RT/b_T (J mol^{-1}) where *R* isthe gas constant (8.314 J $mol^{-1}K^{-1}$), $b_T$is the Temkin isotherm constant and *T* is the absolute temperature (K). B and K_t (L g^{-1}) which is the equilibrium potential corresponding to maximum binding energy can be determined from the linear plot (Tempkin and Pyzhev 1940).

Kinetics study

The experiments were conducted at equilibrium conditions for kinetic modeling. At certain preset time intervals, the aqueous samples were analyzed to determine the concentrations of Ni(II) ions by spectrophotometer. The two kinetic models, namely, pseudo-first order (Lagergren kinetic model) and pseudo-second order model (Ho kinetic model) were used in this study to analyze metal uptake during adsorption.

The first order rate constant for adsorption of Ni(II) has been studied with the help of Lagergran's equation (Lagergren 1898).

$$\log(q_e - q) = log q_e - \frac{k_1 t}{2.303} \quad --6$$

whereqe = the amount of metal adsorbed at equilibrium (mg g^{-1}), q = amount of metal adsorbed at time t (mgg-1), k_1 = first order rate constant of adsorption (per minute) and t = time (minute).

Pseudo-second order rate equation (Ho and McKay 1999):

$$\frac{t}{q_t} = \frac{1}{k_2 q_e^2} + \frac{1}{q_e} t \quad --7$$

where, k_2 = second order rate constant for adsorption (g mg^{-1} min^{-1}), q_e is the amount of Ni(II)ions adsorbed at equilibrium (mg g^{-1}) and q_t = amount of Ni(II) ions adsorbed in time t (min^{-1}). In order to obtain the rate constant, a graph was plotted betweent/$q_t$vs t (Asha *et al*., 2011, Chinenye *et al*., 2016).

Intraparticle diffusion method

Intraparticle diffusion involves the movement of species from the liquid phase to the solid phase. The batch studies confirm the adsorption process taking place on the permeable mesolite.

$$q_t = k_{id} t^{1/2} + C_i \quad --8$$

where, k_{id} ($mgg^{-1}(min)^{½}$) represents intraparticle diffusion rate constant, t denotes contact time (min) and C_i is intraparticle diffusion constant i.e. intercept of the line (mgg^{-1}). It is directly proportionalto the boundary layer thickness. The rate constant was calculated by plotting a graph between the amount of adsorbate, qt (mgg-1) and the square root of the time (qtvs $t^{½}$) gives the rate constant (slope of the plot) (Weber and Morris 1963, Itodo *et al*., 2010).

RESULTS AND DISCUSSION

Characterization of mesolite

Natural mesolite contains a complement of exchangeable sodium, potassium, and calcium ions in an organic matrix (Erdem *et al*., 2004). The characteristics of the mesolite sample (Table 1) are given as follows. The present study demonstrates to assess the potential of mesolitein removing Ni (II) ions from aqueous solution. The pH value (9.0), electrical conductivity (2.01dSm^{-1}) and the water holding capacity (56.35) indicate the good adsorptive capacity of the mesolite. The particle size ratio of mesolite is found to be 1.00 and the results of important characteristics of the mesolite have been discussed in our previous study (Vidhya *et al*., 2016).

Table 1 Characteristics of Mesolite

Characteristics of Biochar	Values
pH	9.3
EC (ds/m)	2.01
Water holding capacity (%)	56.35
Zeta potential (mV)	-5.6
Particle size (SP Area ratio)	1.00
Mean (nm)	378
Standard Deviation (nm)	31.5
Mode (nm)	376

The scanning electron micrograph of the mesolite is depicted in the Fig 1a. The mesolite has several mesopores over the surface and uniform morphology, which has a crucial role in many liquid-solid adsorption processes (Deveci and Kar, 2013, Ahmed *et al*., 2015). The porous nature of the mesolite was not altered after Ni adsorption process (Fig. 1b) suggesting that it can be used as an adsorbent in liquid-solid adsorption process.

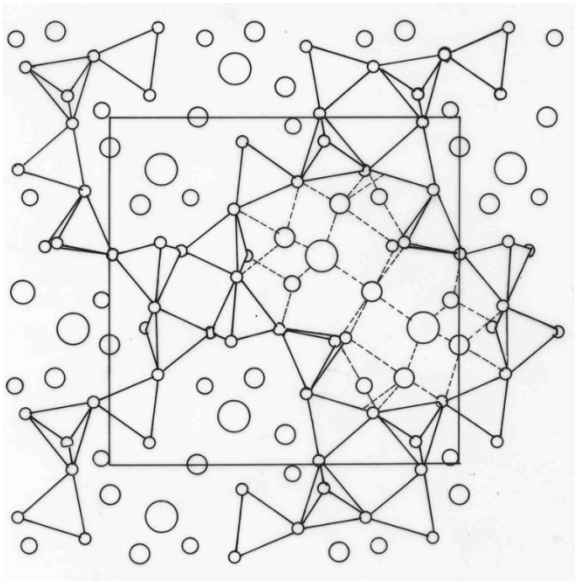

Fig 1a

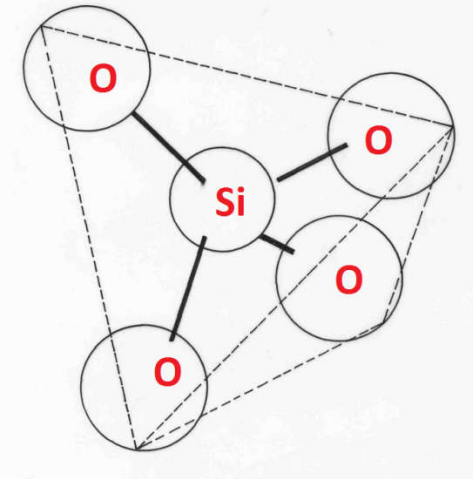

Fig. 1b

Fig 1 a) Chain structure of mesolite b) Tetrahedral arrangement in individual mesolite moiety.

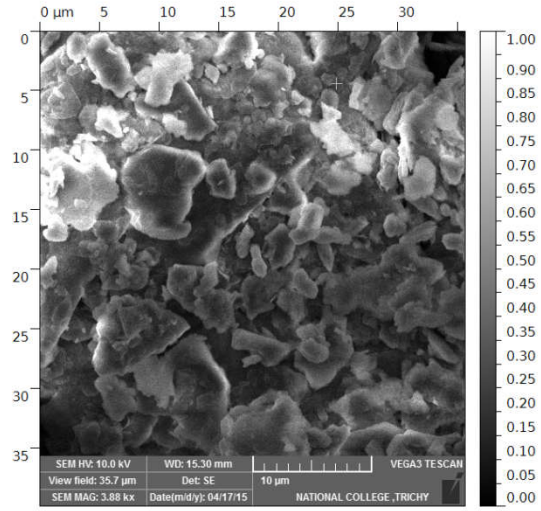

Fig 2a

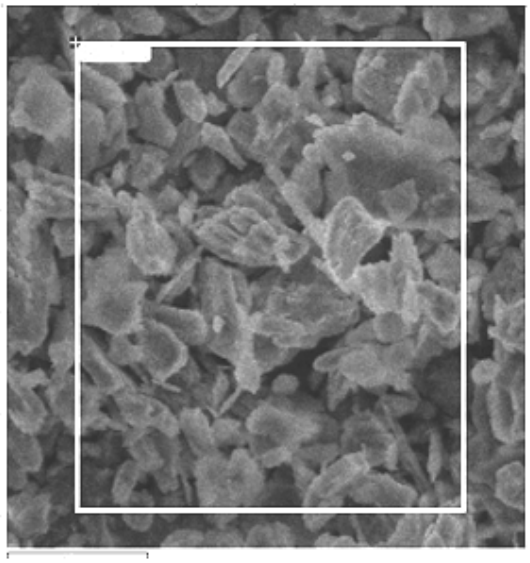

Fig 2b

Fig 2 Scanning electron micrographs of mesolite before and after Ni(II) adsorption. The mesolite has several mesopores over the surface. a) Before Ni(II) adsorption, b) After Ni(II) adsorption.

The energy dispersive spectra of mesolite before and after Ni adsorption are depicted in Fig. 2a and b. The spectra showed the presence of carbon and potassium in both test and control samples. However, the Ni peak (0.4keV) was observed only in test sample, which confirms that mesolite had adsorbed Ni ions from aqueous solution. Transmission Electron Microscopic (TEM) image of mesolite is given in Fig.3. The images showed that the particle size of the mesolite was 1µm.

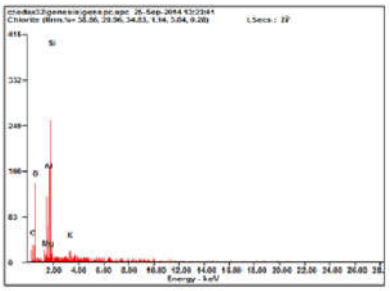

Fig. 3a

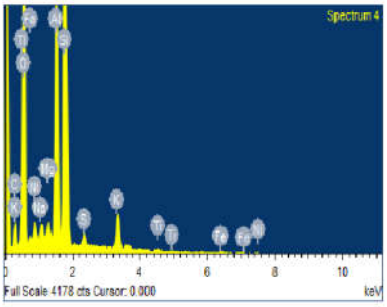

Fig. 3b

Fig 3 SEM-EDS spectra of mesolite before and after Ni(II) adsorption. a) Before Ni(II) adsorption, b) After Ni(II) adsorption.

The SEM and TEM images show that the surface of mesolite had uneven small size particles which revealed a high surface area and porous nature as shown in Fig 2a, 2b and Fig. 4a, 4b. Large surface area of any adsorbent helped to get maximum adsorption (Osikoya *et al*., 2014). FTIR spectral analysis was carried out to find out the changes in the vibrational frequencies of the functional groups of mesolite before and after adsorption of Ni ions, and the results are shown in Fig. 5. In general, the broad band at 3350 to 3700 $cm^{-1}$is credited to Si-OH, Si-OH-Al and-OH hydroxyl groups (Ahamed *et al*., 2015). The broadness of the band indicates inter- and intra-molecular hydrogen bonding in the mesolite (Shin *et al*., 2012). This band also indicates the presence of molecularwater coordinated to the edges of the mesolite channels (Moneimand Ahmed., 2015). The peak was observed both in the free mesoliteas well as the nickel adsorbed mesolite. The frequency at 1874 cm^{-1} indicates the C=O stretching vibration. The bands at 1604 and 1612 cm^{-1}in free and Ni adsorbed spectra are assigned to the characteristic bending vibration of the water molecules attached to frame work (Tabassum *et al*., 2016). The most predominant band occurs at 694 cm^{-1} assigned tentatively to the symmetrical stretching mode of alkyl halide group (Oana *et al*., 2015). Furthermore, the absorption bands at 416 and 462 $cm^{-1}$are assigned to the internal link age vibrations of TO_4 (T=Si or Al) tetrahedral (Moneim and Ahmed, 2015).

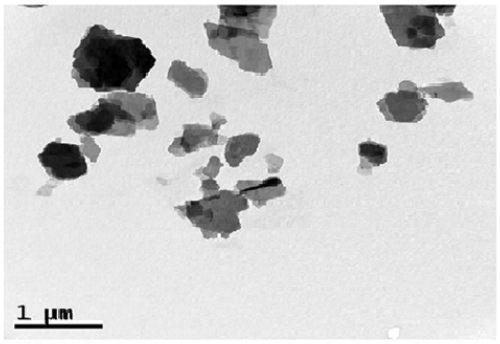

Fig. 4a

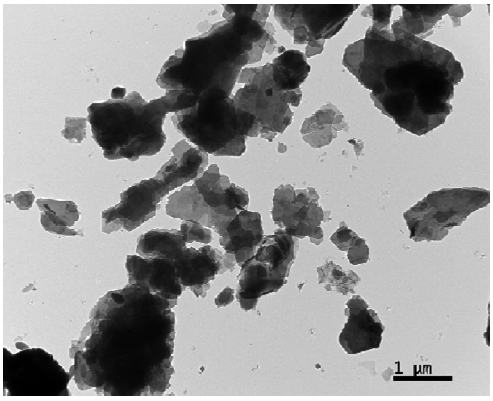

Fig 4b

Fig. 4 Transmission electron micrographs of mesolite before and after Ni(II) adsorption.a) Before Ni(II) adsorption, b) After Ni(II) adsorption.

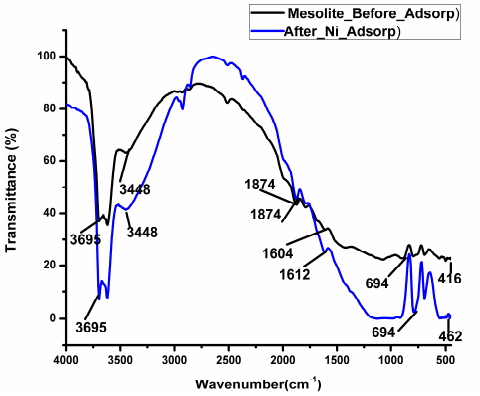

Fig 5

Optimization of initial concentration of Ni (II)

Batch adsorption studies were conducted for the adsorption of Ni(II) onto mesoli teat different initial metal concentrations ranging from 50 to250 mg L^{-1} using 0.05g of mesolite at pH7 (Bennett *et al*., 2013). The results indicated that the percentage of Ni(II) removal was decreased with the increase in initial metal ion concentration (Fig.6a). Due to the limited number of active sites present in the adsorbent, it was saturated at particular concentration (Adhena *et al*., 2014). The maximum percentage of Ni (II) removal observed for mesolite was 99.87%. The initial concentration acts as a driving force to overcome the mass transfer resistance between the solid and liquid phase. Similar occurrence was studied in the adsorption of Ni(II) over marine algae *Gracilaria andits* activated carbon (Esmaeili *et al*., 2011; Vidhya *et al*., 2018). The time required to reach the state of equilibrium was equilibrium time, and it exemplifies the maximum adsorption capacity of the adsorbent. It is obvious from results that the contact time needed to reach the equilibrium condition for Ni(II) was120 min. The results were in alignment with the previous study by Saradhi *et al* (2010) on the biosorption of chromium using sea urchin.

Effect of adsorbent dosage

In order to investigate the effect of adsorbent dose, various amounts of the adsorbent ranging from 0.01g to 0.05g with 100 mg L^{-1}Ni(II) concentration, pH 7 with 120 minequilibration time were used . Increase in adsorption with adsorbent dose (0.01-0.05 g) can be attributed to increased adsorbent surface area and availability of more adsorption sites (Fig.6b) (Dehghani *et al*., 2016). The same trend was observed inthe removal of Cr(VI) using *B. subtilis, Pseudomonas aeruginosa,* and *Enterobacter cloacae* (Sethuraman and Balasubramanian, 2010). It was obvious from the Fig.6b that the removal capacity of Ni(II) is more than 90% in all the dosages. The results are consistent with previous study reporting increased copper adsorption onto natural zeolite (Zendelska *et al*., 2016). The high adsorption was mostly due to the accessibility of more dynamic sites and adsorptive surface area present in the mesolite. From the experiments 0.05 g of the adsorbent dosage was found to be the optimized dosage.

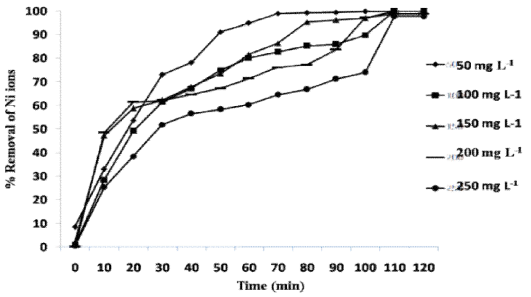

Fig. 6a

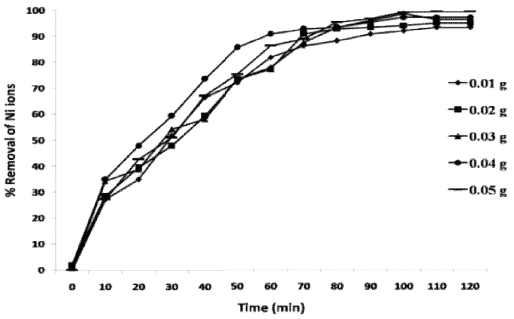

Fig. 6b

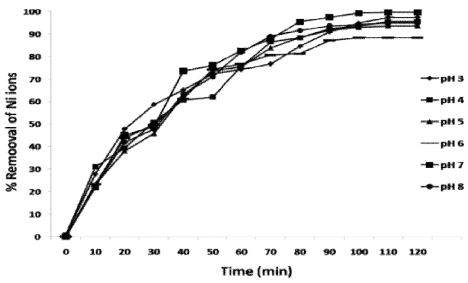

Fig. 6c

Fig 6 a) Effect of initial concentration on adsorption of Ni(II) onto mesolite. The Ni(II) removal was decreased according to the increasing initial concentration. b) Influence of mesolitedosage on adsorption of Ni(II). A minor increase in adsorption efficiency was observed with increase in adsorbent dose. c) Effect of pH on adsorption of Ni(II) onto mesolite. The maximum adsorption (99.6%) was observed at pH 7.

Effect of pH

It is well known that the pH is a vital parameter impacting the adsorption process. It can control metal speciation, mesolite reliability and competence of H^+ ions in ion exchange. The pH of the solution affects the level of adsorption because the distribution of surface charge of the adsorbent can alter thus varying the amount of adsorption (Ibrahimi and Sayyadi., 2015). Exactly 0.05 g of the mesolite was mixed with 25 mL of Ni(II) solutions (100 mg L^{-1}) at different pH values (3-8), and the results are depicted in Fig. 6c**.** It is noticed from Fig. 6c, that sorption of nickel was more than 88% at all pH ranges (3-8). The maximum adsorption of 99.7% was observed at pH 7 (Katsou *et al*. 2010). The results of the present study reveals that the adsorption capacity of Ni(II) increased with the increasing pH which corroborates with the study of Zhang *et al* observation of removal of heavy metal ions using chitosan and modified chitosan.

Adsorption isotherms

The interaction between Ni(II) ions and mesolite was tested by Langmuir, Freundlich and Temkin models The Langmuir isotherm is suitable for monolayer adsorption onto a surface containing a fixed number of the same binding sites. The maximum adsorption occurs when the adsorbent surface is covered by a single molecular layer of soluble material. The adsorption energy is permanent and identical at all the points. The molecules or ions of adsorbed material cannot move in the adsorbent surface (Shidvash *et al*., 2014). The Langmuir isotherms illustrate the RL values indicating whether the isotherm is favorable or not. The RL values should be positioned between 0 and 1.The equation to calculate RL is given as follows.

$$R_L = \frac{1}{(1 + bC_o)}$$

The RL values in the present study are found to be between 0.001 and 0.007 which indicate the isotherm is a favorable one. Langmuir constant (Q_{max}) and Langmuir separation factor (R_L) were used to compare the results and they reflect the adsorption capacity of the adsorbent. Mao *et al*. (2010) reported that the adsorbent with high Q_{max} and RL values is usually advantageous for the wastewater treatment process. The report suggests that the mesolite has higher Q_{max} and the R_L values as compared to the other adsorbents. The Langmuir isotherm model (Fig. 7) fits very well with experimental data (Visa and Popa, 2015; Vidhya *et al*., 2017).

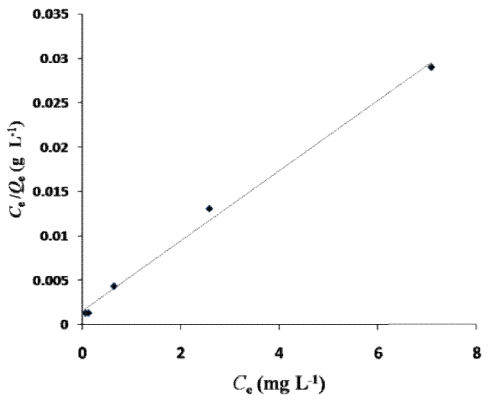

Fig 7 Langmuir Isotherm plot for Ni(II) adsorption onto mesolite.

Freundlich isotherm describes the significance of the factor 1/n which implies the favorability of adsorption. The value of n should either be >1 representing favorable adsorption condition (or) 1/n lying in the range of 1 to 10 confirms the favorable condition for adsorption. High Kf values indicate the high adsorption rate of metal ion due to high compatibility of mesolite towards Ni(II) ions, while low Kf values indicate low adsorption rate of metal ion (Arivoli *et al*., 2012). Table 2 shows that despite the fact that the values of 1/n were good for adsorption of nickel ions, the Kf values of Freundlich isotherm do not fit the adsorption data**.**

The Temkin adsorption isotherm model assesses the adsorption capacity of the adsorbent for the adsorbate. The Temkin isotherm plot for the nickel (II) ions and the parameters are given in Table 2. The results show that Temkin adsorption isotherm does not fit the adsorption data for the sorption of nickel (II) from aqueous solution using mesolite. A comparison of results obtained for Langmuir, Freundlich and Temkin isotherms are presented in Table 2.A comparison of results of the R^2values (Correlation coefficient) of Langmuir, Freundlich and Temkin isotherm model are presented in Table 2. The Langmuir plot shows the R^2values 0.99 close to unity, indicating isotherm data fitted well to Langmuir model and it proceeds by mono layer sorption formation (Sukumar *et al*., 2014; Khalil *et al* ., 2016; Ossman *et al*., 2016).

Table 2 Isotherm model constants for Ni(II) ion adsorption onto Mesolite

Isotherm models	Parameters	Mesolite
Langmuir model	q_m(mg g^{-1})	252.6681
	b (L mg^{-1})	2.668675
	R^2	0.99475
Freundlich model	K_F (mg g^{-1}) (L mg^{-1}) $^{1/n}$	1.383035
	n	0.32428
	R^2	0.907132
Temkin model	K_T	73.13613
	B_T	38.71737
	R^2	0.987072

Kinetic model

Different kinetic models are used in general to illustrate the adsorption capacity, the adsorbate effectiveness, and the adsorption mechanisms. Hence, the equilibrium data were analyzed with the usual pseudo first-order and pseudo second-order kinetic models. Adsorption rate constants and their correlation coefficients (R^2) were calculated from the curves and are summarized in the Table 3. The kinetic data shows that the correlation coefficient for the pseudo first-order kinetic model is very low, indicating a poor fit of the model to the experimental data.

Table 3 Adsorption kinetic model constants for Ni(II) adsorption onto Mesolite

Kinetic models	Parameters	Initial Concentration (mg L^{-1})				
		Mesolite				
		50	100	150	200	250
Pseudo first order	q_e (exp) (mg g-^{1})	49.9355	99.871	149.678	199.355	244.195
	q_e (calc) (mg g^{-1})	96.2426	122.596	116.065	124.246	145.221
	K_1 (min^{-1})	-0.05081	-0.03317	0.03821	-0.03497	-0.03019
	R^2	0.850031	0.833316	0.950804	0.789237	0.649223

	q_e(exp)(mg g-1)	49.9355	99.871	149.6775	199.355	244.195
	q_e(max)(mg g-1)	57.07042	111.4533	166.2526	208.7674	221.2676
Pseudo second order	k_2 (g mg-1 min^{-1})	0.001191	0.000415	0.0003654	0.000278	0.000218
	R^2	0.976489	0.959202	0.968904	0.939285	0.96028
	h	0.067947	0.04631	0.060747	0.058049	0.048157
	k_{id}	4.478839	8.931507	12.88273	15.79354	20.33212
Intra Diffusion method	R^2	0.914262	0.973426	0.964194	0.927516	0.947238
	C	7.691039	6.019299	19.87908	27.0008	1.891304

However, the correlation coefficient value of pseudo second-order model (R^2 = 0.97) (Fig. 8a) was close to unity, indicating the better fit (Noshabah Tabassum *et al*., 2016). Besides, the theoretical values of the q_e calculated from the pseudo second-order model were close to the experimental uptake values of q_{exp} (Barati-Harooni *et al*., 2016).

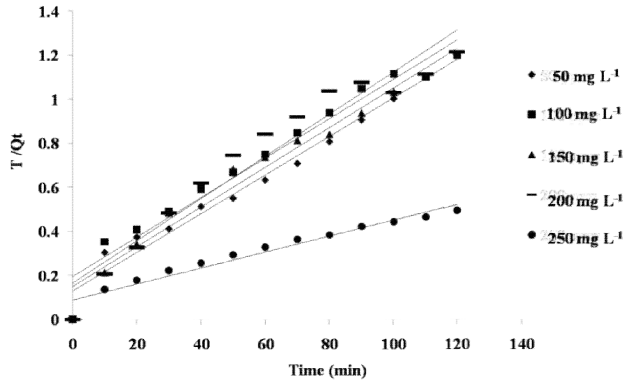

Fig. 8a

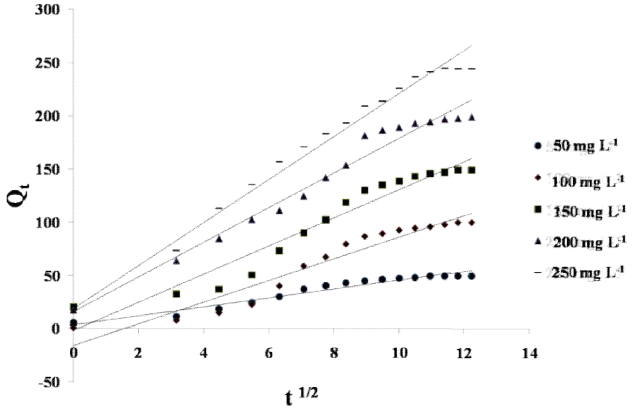

Fig. 8b

Fig 8 a) Pseudo second-order kinetic plot for adsorption of Ni(II) onto mesolite. b) Intra particle method for adsorption of Ni(II) onto mesolite.

Further, this modelhas the correlation coefficient value (R^2= 0.97) which well fitted to the adsorption data (Fig. 8b).The results of the kinetic analysis indicate that the rate of the adsorption was controlled by the chemisorption processes. The results are in accordance with previous study reporting that the pseudo second order kinetic model was found appropriate for the prediction of the binding affinity (Elvis *et al*., 2014).

CONCLUSION

The present study assesses the use of mesolite for the removal of Ni (II) from aqueous solution. The characterization of mesolite demonstrated the adsorption capacity through pH and zeta potential of the adsorbent. The SEM and TEM analysis proves that the surface of the mesolite has good number of pores or sites available for adsorption**.** The ionic interaction between the Ni(II) and functional groups present in the mesolite was established by FTIR studies. The removal of Ni (II) was found to be dependent on different parameters such as adsorbent dose, contact time, pH, and initial concentration. The optimization study signifies that the removal was more than 99%of Ni (II) with the concentration of 100ppm at pH 7 after 120 min. The adsorption data befittingly match the Langmuir isotherm. The adsorption of Ni (II) ions by mesolite followed the pseudo second order kinetics and intraparticle diffusion method. The results indicate that mesolite is an efficient and in-expensive adsorbent that can be used for removal of NI (II) ions from industrial effluents.

Acknowledgement

The first author is grateful to the Departments of Environmental Science of the PSG College of Arts and Science, Coimbatore, Tamil Nadu Agricultural University, Coimbatore, Dr. Kamal-Kannan, Division of Biotechnology, Chonbuk National University and the Department of Chemistry, National College, Thiruchirapalli for providing facilities and extending cordial gestures during the course for her doctoral programme through this study.

References

1. Adhena Ayaliew Werkneh, Nigus Gabbiye Habtu, Hayelom Dargo Beyene (2014) Removal of hexavalent chromium from tannery wastewater using activated carbon primed from sugarcane bagasse: Adsorption/desorption studies. *Amer J App Chem*, 2(6): 128-135.
2. Afrodita Zendelska, Mirjana Golomeova, Krsto Blazev, Boris Krstev, Blagoj Golomeov, Aleksandar Krstev (2015) Adsorption of Copper ions from aqueous solutions on natural zeolites. *Environ Protect Eng* 41(4): 1-36.
3. Ahmed M. Abbas, Yousif I. Mohammed and Taki A. Himdan (2015) Adsorption Kinetic and Thermodynamic Study of Congo Red Dye on Synthetic Zeolite and Modified Synthetic Zeolite. *J. Pure & Appl. Sci.,* 28 (1): 54-72.
4. Ali Barati-Harooni, Adel Najafi-Marghmaleki, Afshin Tatar, Amir H. MohammadiTarek E. Khalil , Ali El-Dissoukya, SayedRizk (2016) Equilibrium and Kinetic studies on Pb^{2+}, Cd^{2+}, Cu^{2+} and Ni^{2+} Adsorption from aqueous solution by Resin 2, 2'-(Ethylenedithio)diethanol Immobilized Amberlite XAD-16 (EDTDE-AXAD-16) with Chlorosulphonic acid. J. *Mol Liq.,* 219: 533-546.
5. APHA (2005) Standard Methods for the Examination of Water and Wastewater. Analytical Public Health Association, Centennial Edition, Washington DC.
6. Arivoli S, Marimuthu V, Ravichandran T and Hema. M (2012) Kinetic, Equilibrium and Mechanistic Studies of Nickel Adsorption on a low cost activated Calcite powder. *Ind. J. Sci. Res. and Tech*., 1(1):41-49. ISSN:-2321-9262 (Online) available at: http://www.indjsrt.com.
7. Asha Gupta, ReenaYadav & Parmila Devi. (2011). Removal of hexavalent chromium using activated

coconut shell and activated coconut coir as low cost adsorbent. *The IIOAB Journal* 2(3), 8-12.

8. Bennett RM, Cordero PRF, Bautista GS & Dedeles GR (2013) Reduction of hexavalent chromium using fungi and bacteria isolated from contaminated soil and water samples, *Chem Ecol.,* 29(4): 320-328.
9. Cheraghi E, Amer E, Moheb A (2015) Adsorption of cadmium ions from aqueous solutions using sesame as a low-cost biosorbent: kinetics and equilibrium studies, *Inter J. Env. Sci Tech.*,12(8) : 2579-2592
10. Chinenye Adaobi Igwegbe, Pius Chukwukelue Onyechi, Okechukwu Dominic Onukwuli, Ikenna Chukwudi Nwokedi (2016) Adsorptive Treatment of Textile Wastewater Using Activated Carbon Produced from Mucunapruriens Seed Shells. *World J. Eng & Technol.,* 4: 21-37.
11. Cybelle Morales Futalan, Chi-Chuan Kan, Maria Lourdes P, Dalida, Chelo Pascua, Kuo-Jung Hsien and Meng-Wei Wan (2011) Nickel removal from aqueous solution in fixed bed using chitosan-coated bentonite, *Sustain Environ Res* 21(6) : 361-367.
12. Dajana Kučić, Marinko Markić, Felicita Briški (2012) Ammonium Adsorption on Natural Zeolite (Clinoptilolite): Adsorption Isotherms and Kinetics Modeling, *The Holistic Appro. Environ* 24:145-158.
13. Deveci H and Kar Y (2013) Adsorption of hexavalent chromium from aqueous solutions by bio-chars obtained during biomass pyrolysis, *J Ind Eng Chem.,* 19:190-196.
14. Elvis Fosso-Kankeu, Magdali Reitz and FransWaanders (2014) Selective Adsorption of Heavy and Light Metals by Natural Zeolites, 6th Int'l Conf. on Green Technology, Renewable Energy & Environmental Engg. (ICGTREEE'2014) Cape Town (SA).
15. Erdem E, Karapinar N, Donat R (2004) The removal of heavy metal cations by natural zeolites. *J. Coll. Interface Sci*., 280: 309-314.
16. Esmaeili A, Beirami P and Ghasemi S (2011) Evaluation of the Marine Algae Gracilaria and its Activated Carbon for the Adsorption of Ni(II) from Wastewater, *E-Journal Chem* http://www.e-journals.net 8(4): 1512-1521.
17. Franus W, Wdowin M (2010) Removal of ammonium ions by selected natural and synthetic zeolites. *Min Res Manage.,* 26(4):133-148.
18. Freundlich, (1906) Hüber die adsorption in Losungen, Engelmann.
19. Gönen F and Onalan F (2016) Adsorptive Removal Behaviour of Procion MX-R Dye from SRDW by Chitosan, *Appl Eco and Environ Res.,* 14(1): 77-98.
20. Ho YS, McKay G (1999) A kinetic study of dye sorption by biosorbent waste product - pith *Res Conserv Recycl.,* 25:171-193.
21. Ho YS, McKay G. (1999) Comparative sorption kinetic studies of dye and aromatic compounds onto fly ash. *Sci. Health Part A*, 34: 1179-1204.
22. Huang K, Xiu H, Zhu Y (2015) Removal of hexavalent chromium from aqueous solution by crosslinkedmangosteenpeelbiosorbent, *Int J. Environ Sci and Technol.,* 12(8) 2485-2492.
23. IkennaChukwudiNwokedi, Adsorptive Treatment of Textile Wastewater Using Activated Carbon Produced from Mucunapruriens Seed Shells, *World J. Eng & Technol.,* 4: 21-37.
24. Itodo AU, Abdulrahman FW, Hassan LG, Maigandi SA, Itodo HU (2010) Intraparticle Diffusion and Intraparticulate Diffusivities of Herbicide on Derived Activated Carbon, *Researcher* 2(2) : 74-86.
25. Karim Zare, Hamidreza Sadegh, Ramin Shahryari-ghoshekandi, Mohammad Asif, Inderjeet Tyagi, Shilpi Agarwal, Vinod Kumar Gupta (2015) Equilibrium and kinetic study of ammonium ion adsorption by Fe3O4 nanoparticles from aqueous solutions, *J. Mol. Liq.,* 213: 345-350.
26. Katsou, E., Malamis, S., Haralambous, K., J and Loizidou, M. (2010). Use of ultrafiltration membranes and aluminosilicate minerals for nickel removal from industrial wastewater. *J Membr. Sci.,* 360, 234-249.
27. Khalil TE, El-Dissouky A, Rizk S (2016) Equilibrium and kinetic studies on Pb^{2+}, Cd^{2+},Cu^{2+} and Ni^{2+} adsorption from aqueous solution by resin 2, 2′-(ethylenedithio) diethanol immobilized amberlite XAD-16 (EDTDE-AXAD-16) with chlorosulphonic acid, *J. Mol. Liq.* 219: 533-546.
28. Lagergren S, and Vetenskapsakademiens KS (1898) Zurtheorie der Sogenannten Adsorption Gelöster Stoffe Kungliga Svenska Vetenskapsakademiens-*Handlingar*, 24(1): 39.46.
29. Langmuir, I. (1918) The adsorption of gases on plane surfaces of glass mica and platinum, *J. Am. Chem. Soc.,* 40:1361-1403.
30. Lata .S, Singh P.K,Samadde S.R (2015) Regeneration of adsorbents and recovery of heavy metals: a review *Int J. Environ Sci Technol.,* 12(4) 1461-1478.
31. Lei Zhang, Yuexian Zeng, Zhengjun Cheng (2016) Removal of heavy metal ions using chitosan and modified chitosan: review *J Molec Liq.,* 214: 175-191.
32. Mao, j., Won, SW., Vijayaraghavan, K., and Yun, YS. (2010). Immobilized citric acid-treated bacterial biosorbents for the removal of cationic pollutants, *Chem Eng. J.* 162: 662-668.
33. Maria Visa and Nicoleta Popa (2015) Adsorption of Heavy Metals Cations onto Zeolite Material from Aqueous Solution,*J Membra Sci Technol.*, 5: 133. http://dx.doi.org/10.4172/2155-9589.1000133.
34. Mohammad Hadi Dehghani, Daryoush Sanaei, Imran Ali , Amit Bhatnagar (2016) Removal of chromium(VI) from aqueous solution using treated waste newspaper as a low-cost adsorbent: Kinetic modeling and isotherm studies, *J Molecular Liq.,* 215: 671-679.
35. Moneim M.A. and Ahmed E.A. (2015) Synthesis of Faujasite from Egyptian Clays: Characterizations and Removal of Heavy Metals. *Geo mat* 5:68-76. http://dx.doi.org/10.4236/gm.2015.52007.
36. Muhammad Mahmood Ibrahimi, Azam Salih Sayyadi (2015) Application of natural and modified Zeolites in removing heavy metal Cations from aqueous media: an overview of including parameters affecting the process, *Int J Geo, Agri & Environ Sci.,* 3(2): 2348-0254.
37. Noshabah Tabassum, Uzaira Rafique and Muhammad Aqeel Ashraf (2016) Metal Doped Green Zeolites for Waste Water Treatment: A Sustainable Remediation Model *J. Chem Soc Pak.,* 38(3):424-437.

38. Nurzulaifa Shaheera Erne Mohd Yasim, Zitty Sarah Ismail, Suhanom Mohd Zaki, Mohd Fahmi AbdAzis, (2016) Adsorption of Cu, As, Pb and Zn by Banana Trunk. *Malay J Anal Sci*, 20 (1): 187 - 196.
39. Oana Lelia Pop, Zorița Diaconeasa, Amalia Mesaroș , Dan Cristian Vodnar, Lucian Cuibus, Lelia Ciontea, Carmen Socaciu (2015) FT-IR Studies of Cerium Oxide Nano particles and Natural Zeolite Materials, *Bulletin UASVM Food Sci & Technol.,* 72(1) : 2344-2344.
40. Osikoya A.O, Wankasi D, Vala R.M.K, Afolabi A. S, Dikio E. D (2014) Synthesis, Characterization and Adsorption Studies of Fluorine-Doped Carbon Nanotubes *Digest J Nano mat &Biostruct*9 (3): 1187 - 1197.
41. Ossman M.E, Abdelfatah M and Kiros Y (2016) Preparation, Characterization and Adsorption Evaluation of old Newspaper Fibres using Basket Reactor (Nickel Removal by Adsorption) *Int. J. Environ. Res*., 10(1):119-130.
42. Peng Zhang, Wenjie Ding, Yanjun Zhang, Kanghai Dai and Wei Liu (2014) Heavy metal ions removal from water using modified zeolites, *J Chem Pharma Res.,* 6(11):507-514.
43. Raziyeh Zandipak, Soheil Sobhanardakani (2016) Evaluation of Kinetic and Equilibrium Parameters of NiFe2O4 Nanoparticles on Adsorption of Reactive Orange Dye from Water, *Iranian J Toxicol* 10(2) 51-58.
44. Rohama Gill, Qurat-ul-Ain Nadeem, Raziya Nadeem, Rabia Nazir, Sadaf Nawaz (2014) Biosorption capacity of vegetable waste biomass for adsorption of lead and chromium. *J Biodiversity & Environ Sci*., 5(2): 306-317.
45. Saradhi BV, Rao SRK, Kumar YP, Vijetha P, Rao KV, Kalyani G (2010) Applicability of Freundlich and Langmuir theory for biosorption of chromium from aqueous solution using test of sea urchin. *Int J Chem Eng Res* 2:139-148.
46. Sethuraman. P, Balasubramanian. N (2010) Removal of Cr (VI) from aqueous solution using Bacillus subtilis, Pseudomonas aeruginosa, and Enterobacter cloacae. *Int J Eng Sci Technol* 2:1811-1825.
47. Seliem M.K, Komarneni. S (2016) Equilibrium and kinetic studies for adsorption of iron from aqueous solution by synthetic Na-A zeolites: Statistical modeling and optimization, *Micropor & Mesopor Mat.,* 228: 266-274.
48. Shah, M.A., Tokeer Ahmad., Principles of Nanoscience and Nanotechnology. Narosa Publishing House, New Delhi, 2013.
49. Shidvash Dowlatshahi, Ahmad Reza Haratinezhad Torbati, & Mahshid Loloei. (2014). Adsorption of copper, lead and cadmium from aqueous solutions by activated carbon prepared from saffron leaves, *Environ. Health Eng. Manage J.*, 1, 37-44.
50. Shin M.N, Shim, J, You Y, Myung H, Bang K.S, Cho M, Kamala Kannan S, Oh B.T(2012) Characterization of lead resistant entophytic Bacillus sp. MN3-4 and its potential for promoting lead accumulation in metal hyper accumulator Alnus firma, *J Hazardous Mat.,* 199-200:314-320.
51. Sukumar C, Gowthami G, Nitya R, Janaki V, Seralathan Kamala-Kannan, & Shanthi K (2014) Significance of co-immobilized activated carbon and Bacillus subtilis on removal of Cr(VI) from aqueous solutions, *Environ Earth Sci.,* 72: 839.
52. Tempkin, Pyzhev V, (1940) Kinetics of ammonia synthesis on promoted iron catalyst, *Acta Phys. Chem*. USSR 12: 327-356
53. Vidhya L, Dhandapani M, Shanthi K, Mahimairaja S (2016) Mesolite, a Natural Adsorbent, for the Removal of Hexavalent Chromium (VI) From Aqueous Solutions, *ChemSci Rev Lett.,* 5(18): 151-163.
54. Vidhya L, Dhandapani M, Shanthi K (2017) Sequestering Divalent Nickel Ions from Aqueous Solution Using Activated Carbon of *Citrus limetta* Peel: Isothermic and Kinetic Studies, *Pol. J. Environ. Stud.,* 26 (4): 1737-1745.
55. Vidhya L, Dhandapani M, Shanthi K, Kamala Kannan S (2018)Removal of Cr(VI) from aqueous solution using coir pith biochar - An eco- friendly approach, *Indian J. Chem. Technol.,* 25: 266-273.
56. Weber W.J, Morris J.C (1963) Kinetics of adsorption on carbon from solution- *J. Sanit. Engg. Div* 89: 31-60.

How to cite this article:

Vidhya Lakshmanaperumal and Dhandapani Munusamy., 2019, Assessment of Adsorption Efficiency of Ni (II) IONS From Aqueous Solution By Mesoporous Alumino Silicate Synthesized From Natural Hydrated Sodium Calcium Alumino Silicate. *Int J Recent Sci Res.* 10(07), pp. 33515-33523. DOI: http://dx.doi.org/10.24327/ijrsr.2019.1007.3686

****